

A $1.75 h^{-1}$ KPC SEPARATION DUAL AGN AT $z = 0.36$ IN THE COSMOS FIELD

JULIA M. COMERFORD¹, ROGER L. GRIFFITH², BRIAN F. GERKE³, MICHAEL C. COOPER^{4,5},
JEFFREY A. NEWMAN⁶, MARC DAVIS^{1,7}, AND DANIEL STERN²

¹Astronomy Department, 601 Campbell Hall, University of California, Berkeley, CA 94720

²Jet Propulsion Laboratory, California Institute of Technology, MS 169-327, 4800 Oak Grove Drive, Pasadena, CA 91109

³Kavli Institute for Particle Astrophysics and Cosmology, M/S 29, Stanford Linear Accelerator Center,
2575 Sand Hill Rd., Menlo Park, CA 94725

⁴Steward Observatory, University of Arizona, Tucson, AZ 85721

⁵Spitzer fellow

⁶Department of Physics and Astronomy, University of Pittsburgh, Pittsburgh, PA 15260 and

⁷Department of Physics, University of California, Berkeley, CA 94720

Submitted for Publication in *ApJL*

ABSTRACT

We present strong evidence for dual active galactic nuclei (AGN) in the $z = 0.36$ galaxy COSMOS J100043.15+020637.2. COSMOS *Hubble Space Telescope* (*HST*) imaging of the galaxy shows a tidal tail, indicating that the galaxy recently underwent a merger, as well as two bright point sources near the galaxy's center. Both the luminosities of these sources (derived from the *HST* image) and their emission line flux ratios (derived from Keck/DEIMOS slit spectroscopy) suggest that both are AGN and not star-forming regions or supernovae. Observations from zCOSMOS, Sloan Digital Sky Survey, *XMM-Newton*, Very Large Array, and *Spitzer* fortify the evidence for AGN activity. With *HST* imaging we measure a projected spatial offset between the two AGN of $1.75 \pm 0.03 h^{-1}$ kpc, and with DEIMOS we measure a 150 ± 40 km s⁻¹ line-of-sight velocity offset between the two AGN. Combined, these observations provide substantial evidence that COSMOS J100043.15+020637.2 is a dual AGN in a merger-remnant galaxy.

Subject headings: galaxies: active – galaxies: nuclei

1. INTRODUCTION

In the standard Λ cold dark matter paradigm of structure formation, more massive galaxies are assembled from smaller ones in a series of merger events. Nearly every galaxy hosts a central supermassive black hole (SMBH) (Kormendy & Richstone 1995), which implies that a merger between two galaxies nearly always results in a merger-remnant galaxy containing two SMBHs. Drag from dynamical friction causes the two SMBHs to inspiral toward the center of the merger-remnant. The SMBHs spend ~ 100 Myr at separations $\gtrsim 1$ kpc (Begelman et al. 1980; Milosavljević & Merritt 2001), then form a parsec-scale binary and ultimately coalesce into a single central SMBH in the merger-remnant galaxy. This final coalescence is necessary to preserve the tight observational correlation between the mass of the black hole and the velocity dispersion, or total mass, of the host galaxy stellar bulge (Ferrarese & Merritt 2000).

Although SMBH pairs are a natural consequence of galaxy mergers, there have been few unambiguous detections of galaxies hosting SMBH pairs. If sufficient gas accretes onto both SMBHs, they may each be visible as an active galactic nucleus (AGN). To date, there have been definitive detections of only four galaxies hosting such AGN pairs. First, radio signatures of AGN activity in the $z = 0.055$ elliptical galaxy 0402+379 show that it hosts binary SMBHs separated by $5 h^{-1}$ pc (Xu et al. 1994; Maness et al. 2004; Rodriguez et al. 2006). In addition, X-ray detections of a dual AGN in the $z = 0.024$ ultraluminous infrared galaxy NGC 6240 indicate it hosts two SMBHs separated by $0.5 h^{-1}$ kpc (Komossa et al. 2003). Finally, optical spectroscopic signatures of dual AGN in the red galaxies EGS2 J142033.6+525917 at

$z = 0.71$ and EGS2 J141550.8+520929 at $z = 0.62$ show these galaxies host dual SMBHs at separations of $0.84 h^{-1}$ kpc and $1.6 h^{-1}$ kpc, respectively (Gerke et al. 2007; Comerford et al. 2009). A fifth possible example has been proposed by Boroson & Lauer (2009), though it is likely to be an object of a different nature (e.g., Chornock et al. 2009a,b; Gaskell 2009; Lauer & Boroson 2009; Wrobel & Laor 2009).

Here we present evidence for a $1.75 \pm 0.03 h^{-1}$ kpc projected spatial separation and 150 ± 40 km s⁻¹ line-of-sight velocity separation SMBH pair, visible as the $z = 0.36$ dual AGN system COSMOS J100043.15+020637.2 in the COSMOS field (Scoville et al. 2007b). The candidate was found serendipitously while visually inspecting postage stamp images of COSMOS galaxies with high Sérsic indices in the ACS-GC catalog (Griffith et al., in preparation), which includes morphology measurements for over half a million sources from five large *Hubble Space Telescope* Advanced Camera for Surveys (*HST* ACS) imaging datasets. In addition, the candidate has been previously classified as an AGN by both COSMOS (Gabor et al. 2009) and the Sloan Digital Sky Survey (SDSS) (York et al. 2000; Richards et al. 2002). We assume a Hubble constant $H_0 = 100 h$ km s⁻¹ Mpc⁻¹, $\Omega_m = 0.3$, and $\Omega_\Lambda = 0.7$ throughout, and all distances are given in physical (not comoving) units.

2. OBSERVATIONS

2.1. COSMOS Imaging

We originally identified COSMOS J100043.15+020637.2 as a dual AGN candidate from its *HST* F814W ACS image taken for COSMOS (Scoville et al. 2007a). This image, shown in Figure 1,

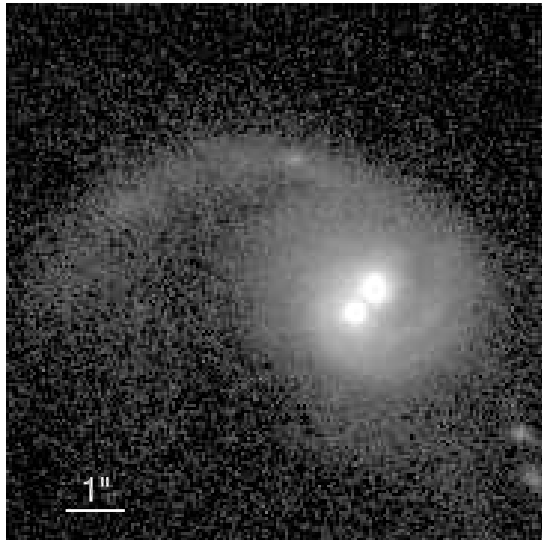


FIG. 1.— *HST* F814W ACS image of COSMOS J100043.15+020637.2, where North is up and East is to the left. The galaxy’s tidal tail strongly suggests it has recently undergone a merger, and the two bright nuclei near the galaxy center appear to both be AGN. The nuclei are separated by $0''.497 \pm 0''.009$, or $1.75 \pm 0.03 h^{-1}$ kpc.

shows a disturbed galaxy with a long tidal tail that suggests the galaxy has recently undergone a merger. The nucleus of the galaxy contains two bright point sources, and we use $0''.25$ ($0.88 h^{-1}$ kpc) radius apertures to measure the magnitude and luminosity of each source with Source EXtractor (Bertin & Arnouts 1996).

We measure F814W apparent magnitudes of 20.0 for the northern source and 20.1 for the southern source. For comparison, the entire object has an apparent magnitude of 18.3, as measured using GALFIT (Peng et al. 2002; Griffith et al., in preparation). The magnitudes of the point sources correspond to luminosities of $3.1 \times 10^{43} h^{-2}$ erg s^{-1} ($8.0 \times 10^9 h^{-2} L_{\odot}$) for the northern source and $2.7 \times 10^{43} h^{-2}$ erg s^{-1} ($7.1 \times 10^9 h^{-2} L_{\odot}$) for the southern source. Supernovae this luminous are extremely rare (Smith et al. 2007), suggesting that the sources are most likely AGN and not supernovae. However, the *HST* image was taken on UT 2004 March 16 and a more recent high-resolution image would resolve this question definitively. Regardless, other observations strongly support the interpretation that both sources are AGN (§ 2.3).

With Source EXtractor we also find that the projected separation between the barycenters of the sources is $0''.497 \pm 0''.009$, or $1.75 \pm 0.03 h^{-1}$ kpc, and the barycenters of the sources are aligned along a position angle $\theta = -40^{\circ}.4$ East of North.

2.2. DEIMOS Slit Spectroscopy

We used the DEIMOS spectrograph on the Keck II telescope to obtain a 200 s spectrum of the object with a 600 lines mm^{-1} grating at twilight on UT 2009 April 23. The spectrum spans the wavelength range 4730–9840 Å, and the position angle of the slit was $\theta = -36^{\circ}.7$ East of North. The main purposes of the slit spectroscopy were to verify that both central point sources were AGN and to measure the spatial and velocity separations between

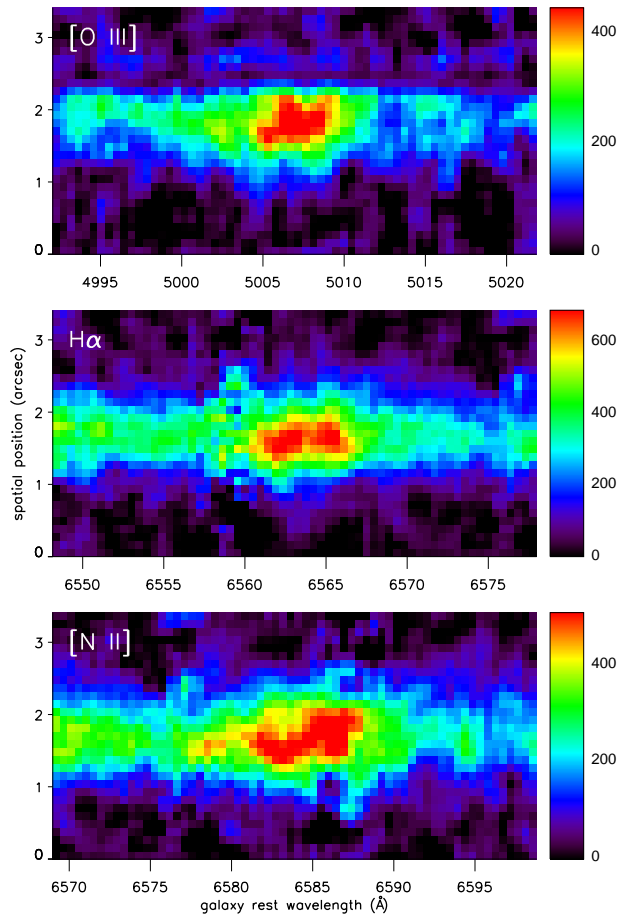


FIG. 2.— Two-dimensional DEIMOS spectrum of J100043.15+020637.2 with night-sky emission features subtracted. The spectrum has been smoothed by a smoothing length of 2 pixels, and AGN line emission at [O III] $\lambda 5007$ (top), H α (middle), and [N II] $\lambda 6584$ (bottom) is shown. In each panel, the vertical axis spans $3''.41$ ($12.0 h^{-1}$ kpc at the $z = 0.36$ redshift of the galaxy) in spatial position along the slit and the horizontal axis spans 30 Å in rest-frame wavelength centered on the emission feature. The color bars provide scales for the flux in counts hour⁻¹ pixel⁻¹. Each emission feature has two components, likely corresponding to two distinct AGN, and the velocity separation between the two is 150 ± 40 km s^{-1} .

the two AGN emission components. The AGN emission is clearly visible in [O III] $\lambda 5007$, H α , and [N II] $\lambda 6584$, as shown in Figure 2. We determine the projected spatial separation for each of these three emission features by measuring the spatial centroid of each emission component individually.

To measure the spatial centroid of an emission component, first we center a 2 Å (rest-frame) wide window on the emission. At each spatial position we then sum the flux, weighted by the inverse variance, over all wavelengths within the window. We use the spatial position where the summed flux is maximum as the center of a 10 pixel window (where 1 DEIMOS pixel spans $0''.11$) around the emission. We then fit a quadratic to the summed flux to locate a peak, define a narrow window centered on the peak flux, and finally compute the line centroid within this window. We derive the error on this spatial centroid by repeatedly adding noise to the spectrum drawn from a Gaussian with variance matching the DEIMOS pipeline (Newman et al., in preparation) esti-

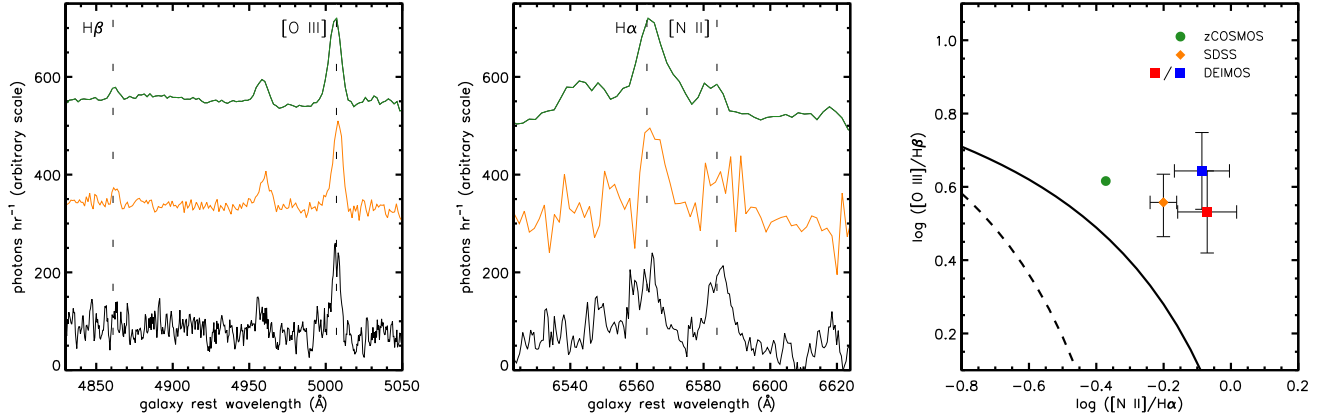


FIG. 3.— Segments of the zCOSMOS (top, green), SDSS (middle, orange), and DEIMOS (bottom, black) spectra and the corresponding BPT diagram for COSMOS J100043.15+020637.2. Each spectrum is shifted to the rest frame of the host galaxy, and the dashed vertical lines show the expected wavelengths of H β and [O III] λ 5007 (left panel) and H α and [N II] λ 6584 (middle panel). For clarity, the spectra are offset from each other vertically and normalized to span 300 counts hr^{-1} . The plotted DEIMOS spectrum has been smoothed by taking the inverse-variance-weighted mean in a rolling 4 \AA wide window. The right panel shows the BPT diagram of the line flux ratios for zCOSMOS (green circle), SDSS (orange diamond), and DEIMOS redward (red square) and blueward (blue square) emission components. The dashed curve illustrates the theoretical maximum for starbursts, based on the upper limit of stellar photoionization models (Kewley et al. 2001), while the solid curve shows the empirical division between galaxies that are purely star-forming and “composite” galaxies whose spectra are dominated by both star formation and AGN (Kauffmann et al. 2003). Pure star-forming galaxies lie under the dashed curve, composite galaxies lie between the dashed and solid curves, and pure AGN galaxies lie above the solid curve. Our line flux ratio measurements of COSMOS J100043.15+020637.2 show that both of its emission components are dominated exclusively by AGN activity.

mate for a given pixel and redoing all centroid measurements.

We find the two AGN emission components have projected separations of $1.5 \pm 0.5 h^{-1}$ kpc, $0.97 \pm 0.42 h^{-1}$ kpc, and $1.6 \pm 0.4 h^{-1}$ kpc in [O III] λ 5007, H α , and [N II] λ 6584, respectively. The low spatial separation measured for the H α emission is due to the imperfectly-subtracted night sky line partially obscuring the blueward portion of the H α emission, but the [O III] λ 5007 and H α spatial offsets are roughly consistent with the spatial offset measured in the *HST* image (§ 2.1). We note that the $3^\circ.7$ difference between the position angle of the DEIMOS slit and the orientation of the two AGN (measured in § 2.1 from the *HST* image) produces a negligible (0.2%) difference between the DEIMOS and *HST* measurements of projected spatial offsets.

2.3. One-Dimensional zCOSMOS, SDSS, and DEIMOS Spectra

We analyze spectra of COSMOS J100043.15+020637.2 from the zCOSMOS spectroscopic redshift survey of the COSMOS field (Lilly et al. 2007), SDSS, and DEIMOS to both determine the galaxy’s redshift and measure emission line flux ratios to determine the source of its line emission.

To measure the redshift of COSMOS J100043.15+020637.2, we determine the value of z which minimizes χ^2 when comparing to a template spectrum. We mask out all emission lines, then fit a continuum template spectrum based on Bruzual & Charlot (2003) stellar-population synthesis models. The template spectrum, described in Yan et al. (2006), consists of a 0.3 Gyr, solar metallicity, young stellar population combined with a 7 Gyr, solar metallicity, old stellar population. From the template spectrum fits, we find that the zCOSMOS, SDSS, and DEIMOS spectra all

give consistent redshifts of $z = 0.36$.

The source of line emission in a galaxy is commonly identified using the Baldwin-Phillips-Terlevich (BPT) diagram of line ratios (Baldwin et al. 1981; Kewley et al. 2006). To determine the source of the line emission in COSMOS J100043.15+020637.2, we examine its H β , [O III] λ 5007, H α , and [N II] λ 6584 emission lines in the zCOSMOS, SDSS, and DEIMOS spectra (Figure 3).

The higher spectral resolution ($R \sim 3000$) of the DEIMOS spectrum enables us to discern substructure in the emission lines that is unresolved in the zCOSMOS and SDSS spectra ($R \sim 600$ and $R \sim 1800$, respectively). To determine the velocity difference between the two peaks we fit two Gaussians to the continuum-subtracted [O III] λ 5007 line profile, which is the emission line with the highest signal-to-noise ratio. Based on the wavelengths of the peaks of the best-fit Gaussians, we find the line-of-sight velocity difference between the double peaks is $150 \pm 40 \text{ km s}^{-1}$. The error in velocity is derived from the errors in the peak wavelengths of the best-fit Gaussians added in quadrature.

To identify whether the double-peaked lines correspond to two AGN, we examine the line flux ratios of each emission component separately. We fit two Gaussians to each double-peaked line, setting the velocity separation of the peaks to the best-fit velocity difference found for the [O III] λ 5007 line profile, but allowing the heights and widths of the Gaussians to vary. The areas under the best-fit Gaussians provide estimates of the line fluxes for each emission component, and we find [O III] λ 5007/H β = 4.4 ± 1.2 and [N II] λ 6584/H α = 0.82 ± 0.17 for the blueward emission component and [O III] λ 5007/H β = 3.4 ± 1.0 and [N II] λ 6584/H α = 0.85 ± 0.19 for the redward emission component, where the uncertainties are derived from propagation of errors in the parameters of the best-fit Gaus-

sians. As Figure 3 shows, the locations of these line flux ratios on the BPT diagram indicate that the line emission for both emission components is clearly produced by AGN activity and not star formation (Kewley et al. 2006). In other words, the combined DEIMOS line flux ratios indicate that COSMOS J100043.15+020637.2 hosts two distinct AGN at nearly the same redshifts.

To measure the line flux ratios for the lower-resolution zCOSMOS and SDSS spectra, we subtract the continuum from each spectrum and then measure the flux of the $H\beta$, $[O III] \lambda 5007$, $H\alpha$, and $[N II] \lambda 6584$ emission lines. For zCOSMOS we measure $[O III] \lambda 5007/H\beta=4.1$ and $[N II] \lambda 6584/H\alpha=0.42$ (we cannot compute errors on these ratios because no error array is provided with public zCOSMOS spectra; however, the error on $[N II] \lambda 6584/H\alpha$ may be large because of the night sky line partially obscuring the $H\alpha$ emission), and for SDSS we measure $[O III] \lambda 5007/H\beta=3.6 \pm 0.7$ and $[N II] \lambda 6584/H\alpha=0.63 \pm 0.06$. The locations of these line flux ratios on the BPT diagram both confirm that the line emission in COSMOS J100043.15+020637.2 is produced by AGN activity (Figure 3).

2.4. Multiwavelength Detections

We use the Infrared Science Archive¹ to obtain additional observations of COSMOS J100043.15+020637.2 across different wavebands, which bolster the evidence for AGN activity found in § 2.1 and § 2.3 as described below.

XMM-Newton detected fluxes of 3.82×10^{-14} erg cm⁻² s⁻¹, 6.08×10^{-14} erg cm⁻² s⁻¹, and 2.87×10^{-14} erg cm⁻² s⁻¹ at energy bands 0.5 – 2.0 keV, 2.0 – 10.0 keV, and 5.0 – 10.0 keV, respectively. These fluxes are above the limit for AGN detection, given by $\sim 10^{-15}$ erg cm⁻² s⁻¹ in the 0.5 – 2.0 keV or 2.0 – 10.0 keV energy bands (Brusa et al. 2007; Cappelluti et al. 2007). In addition, the Very Large Array (VLA) detected a flux of 0.139 mJy at an observing frequency of 1.4 GHz, which is above the limit of 0.1 mJy at 1.4 GHz for AGN detection (Schinnerer et al. 2007). Finally, the *Spitzer* Infrared Array Camera (IRAC) measured Vega magnitudes of 14.92, 14.34, 13.79, and 12.66 at 3.6, 4.5, 5.8, and 8.0 μ m, respectively (Sanders et al. 2007), and these measurements fall within the observed range of mid-infrared colors of AGN (Stern et al. 2005).

These observations, combined with additional data from *Spitzer* MIPS (at 24 and 70 μ m; Sanders et al. 2007), the Canada-France-Hawaii Telescope Legacy Survey² (CFHTLS; in u^* , g' , r' , i' , and z'), SDSS (in u' , g' , r' , i' , and z'), and the *Galaxy Evolution Explorer* (*GALEX*; in the near-ultraviolet and far-ultraviolet) enable us to compile a rest-frame SED for COSMOS J100043.15+020637.2 across several wavebands (Figure 4). This figure also shows the median radio-loud and radio-quiet QSO SEDs compiled by Elvis et al. (1994), and a Bruzual & Charlot (2003) template SED for a 100-Myr-old simple stellar population with metallicity of 0.02 times the Solar value. The QSO templates have been normalized to the 24 μ m detection and the stellar template has been normalized to the z' -band detection. The SED of this object is broadly consistent with a QSO that is

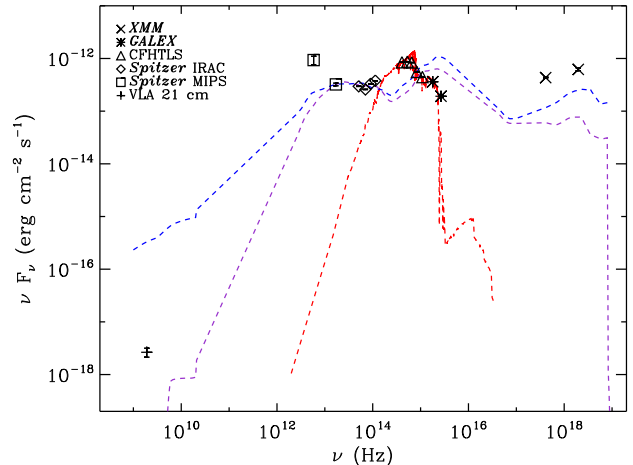


FIG. 4.— SED of COSMOS J100043.15+020637.2, from radio to X-ray. Data points show fluxes (or upper limits) measured by various instruments, as noted in the legend. All frequencies have been shifted to the host galaxy’s rest frame. Also shown are the Elvis et al. (1994) median SEDs for radio-loud and radio-quiet QSOs (blue and purple, respectively) normalized to the 24-micron flux, as well as a Bruzual & Charlot (2003) template SED for a 100-Myr-old stellar population (red) normalized to the z' -band flux.

obscured by dust in the optical and UV, allowing stellar emission from the host galaxy to dominate, with strong re-radiation by dust in the mid-infrared. Some or all of the infrared radiation might also arise from ongoing star formation, as a merger like this one would be expected to produce strong nuclear starbursts, but the X-ray and radio detections confirm the presence of at least one active nucleus in this system.

3. CONCLUSIONS

The observations discussed here provide strong evidence for a dual AGN with $1.75 \pm 0.03 h^{-1}$ kpc projected spatial separation and 150 ± 40 km s⁻¹ line-of-sight velocity separation in the $z = 0.36$ galaxy COSMOS J100043.15+020637.2. The $[O III] \lambda 5007/H\beta$ and $[N II] \lambda 6584/H\alpha$ line flux ratios of the DEIMOS double-peaked emission lines are solid indicators that the galaxy hosts two AGN, a conclusion that is bolstered by the AGN-like luminosities of the galaxy’s two central point sources. Line flux ratios of the unresolved, combined emission lines in zCOSMOS and SDSS spectra, as well as X-ray, radio, and infrared detections, provide further confirmation of AGN activity in the galaxy. Finally, the tidal tail visible in *HST* imaging is an unmistakable signature of a galaxy merger. We conclude that COSMOS J100043.15+020637.2 is a merger-remnant galaxy with two inspiralling supermassive black holes, each of which powers an AGN.

The discovery of this dual AGN adds significantly to the number of such known objects. A statistical sample of dual AGN would provide a direct observational probe of both the galaxy merger rate and the kinematics of SMBH mergers, which are expected to produce gravity waves observable by next-generation projects such as LISA (Bender et al. 1998).

We initially identified COSMOS J100043.15+020637.2 as a dual AGN candidate because of its two bright cen-

¹ <http://irsa.ipac.caltech.edu/>

² <http://www.cfht.hawaii.edu/Science/CFHTLS/>

tral sources visible in *HST* imaging. Our finding was serendipitous, and there are likely more dual AGN to be discovered in COSMOS. We have demonstrated that dual AGN candidates can be selected as bright double sources in *HST* imaging and confirmed through optical spectroscopy and multiwavelength observations.

J.M.C. acknowledges support from NSF grant AST-0507428. The work of R.L.G. and D.S. was carried out at the Jet Propulsion Laboratory at the California Institute of Technology, under a contract with NASA. B.F.G. acknowledges support by the U.S. Department of Energy under contract number DE-AC3-76SF00515. M.C.C. was supported by NASA through the Spitzer Space Telescope Fellowship program. We thank Hai Fu for valuable assistance with the zCOSMOS spectrum.

This letter is partly based on observations carried out using MegaPrime/MegaCam, a joint project of CFHT and CEA/DAPNIA, at the CFHT which is operated by the NRC of Canada, the Institut National des Science

de l'Univers of the CNRS of France, and the University of Hawaii; *GALEX*, a NASA funded Small Explorer Mission; SDSS and SDSS-II, which are funded by the Alfred P. Sloan Foundation, the Participating Institutions, the NSF, the US Department of Energy, NASA, the Japanese Monbukagakusho, the Max Planck Society, and the Higher Education Funding Council for England; the *Spitzer Space Telescope*, which is operated by the Jet Propulsion Laboratory, California Institute of Technology under a contract with NASA; the VLA, a facility of the NRAO, itself a facility of the NSF that is operated by Associated Universities, Inc.; *XMM-Newton*, an ESA science mission with instruments and contributions directly funded by ESA Member States and the USA (NASA); and the W.M. Keck Observatory. We wish to recognize and acknowledge the very significant cultural role and reverence that the summit of Mauna Kea has always had within the indigenous Hawaiian community. We are most fortunate to have the opportunity to conduct observations from this mountain.

REFERENCES

- Baldwin, J. A., Phillips, M. M., & Terlevich, R. 1981, *PASP*, 93, 5
 Begelman, M. C., Blandford, R. D., & Rees, M. J. 1980, *Nature*, 287, 307
 Bender, P., et al. 1998, *LISA Pre-Phase: A Report*, 2nd ed.
 Bertin, E., & Arnouts, S. 1996, *A&AS*, 117, 393
 Boroson, T. A., & Lauer, T. R. 2009, *Nature*, 458, 53
 Brusa, M., et al. 2007, *ApJS*, 172, 353
 Bruzual, G., & Charlot, S. 2003, *MNRAS*, 344, 1000
 Cappelluti, N., et al. 2007, *ApJS*, 172, 341
 Chornock, R., et al. 2009a, *The Astronomer's Telegram*, 1955, 1
 —. 2009b, *ArXiv e-prints*
 Comerford, J. M., et al. 2009, *ApJ*, 698, 956
 Elvis, M., Wilkes, B. J., McDowell, J. C., Green, R. F., Bechtold, J., Willner, S. P., Oey, M. S., Polomski, E., & Cutri, R. 1994, *ApJS*, 95, 1
 Ferrarese, L., & Merritt, D. 2000, *ApJ*, 539, L9
 Gabor, J. M., et al. 2009, *ApJ*, 691, 705
 Gaskell, C. M. 2009, *ArXiv e-prints*
 Gerke, B. F., et al. 2007, *ApJ*, 660, L23
 Kauffmann, G., Heckman, T. M., Tremonti, C., Brinchmann, J., Charlot, S., White, S. D. M., Ridgway, S. E., Brinkmann, J., Fukugita, M., Hall, P. B., Ivezić, Ž., Richards, G. T., & Schneider, D. P. 2003, *MNRAS*, 346, 1055
 Kewley, L. J., Dopita, M. A., Sutherland, R. S., Heisler, C. A., & Trevena, J. 2001, *ApJ*, 556, 121
 Kewley, L. J., Groves, B., Kauffmann, G., & Heckman, T. 2006, *MNRAS*, 372, 961
 Komossa, S., Burwitz, V., Hasinger, G., Predehl, P., Kaastra, J. S., & Ikebe, Y. 2003, *ApJ*, 582, L15
 Kormendy, J., & Richstone, D. 1995, *ARA&A*, 33, 581
 Lauer, T. R., & Boroson, T. A. 2009, *ArXiv e-prints*
 Lilly, S. J., et al. 2007, *ApJS*, 172, 70
 Maness, H. L., Taylor, G. B., Zavala, R. T., Peck, A. B., & Pollack, L. K. 2004, *ApJ*, 602, 123
 Milosavljević, M., & Merritt, D. 2001, *ApJ*, 563, 34
 Peng, C. Y., Ho, L. C., Impey, C. D., & Rix, H.-W. 2002, *AJ*, 124, 266
 Richards, G. T., et al. 2002, *AJ*, 123, 2945
 Rodriguez, C., Taylor, G. B., Zavala, R. T., Peck, A. B., Pollack, L. K., & Romani, R. W. 2006, *ApJ*, 646, 49
 Sanders, D. B., et al. 2007, *ApJS*, 172, 86
 Schinnerer, E., et al. 2007, *ApJS*, 172, 46
 Scoville, N., et al. 2007a, *ApJS*, 172, 38
 —. 2007b, *ApJS*, 172, 1
 Smith, N., Li, W., Foley, R. J., Wheeler, J. C., Pooley, D., Chornock, R., Filippenko, A. V., Silverman, J. M., Quimby, R., Bloom, J. S., & Hansen, C. 2007, *ApJ*, 666, 1116
 Stern, D., et al. 2005, *ApJ*, 631, 163
 Wrobel, J. M., & Laor, A. 2009, *ArXiv e-prints*
 Xu, W., Lawrence, C. R., Readhead, A. C. S., & Pearson, T. J. 1994, *AJ*, 108, 395
 Yan, R., Newman, J. A., Faber, S. M., Konidaris, N., Koo, D., & Davis, M. 2006, *ApJ*, 648, 281
 York, D. G., et al. 2000, *AJ*, 120, 1579